Thermal Decomposition of 2-Fluoroethanol: Single Pulse Shock Tube and ab Initio Studies

B. Rajakumar,[†,#] K. P. J. Reddy,[‡] and E.Arunan*[,†]

Department of Inorganic and Physical Chemistry and Department of Aerospace Engineering, Indian Institute of Science, Bangalore 560012, India

Received: October 28, 2002; In Final Form: September 8, 2003

The thermal decomposition of 2-fluoroethanol (FEOH) has been studied in the temperature range of 1000−1200 K behind reflected shock waves in a single pulse shock tube. The total pressures behind the reflected shocks varied between 13 and 23 atm. The products observed in the covered temperature range are CH_3CHO, C_2H_3F, CH_4, CO, C_2H_4, and C_2H_6. The unimolecular eliminations of HF and H_2O are found to be the major channels through which 2-fluoroethanol decomposes under these conditions. The rate constant for HF elimination is found to be $10^{13.17\pm0.33}$ exp[−(59.5 ± 1.7)/(*RT*)] s^{-1}, and the rate constant for H_2O elimination is found to be $10^{14.30\pm0.34}$ exp[−(69.7 ± 1.7)/(*RT*)] s^{-1}, where the activation energies are given in kcal mol^{-1}. The CH_3CHO produced by HF elimination through the vinyl alcohol intermediate is chemically active and decomposes leading to CH_4 and CH_3CH_3 products. The production of ethylene could not be explained from the CH_3CHO pyrolysis mechanism. It is most likely formed directly from the reactant through HOF elimination or by radical processes beginning with C−O bond dissociation. Ab initio (Hartree−Fock [**HF**] and second-order Møller−Plesset perturbation theory [MP2]) and density functional theory [DFT] calculations have been carried out to find the transition state and activation barrier for HF and H_2O elimination reactions. The **HF** calculations overestimate the barrier by 18 kcal mol^{-1} for HF elimination and 22 kcal mol^{-1} for H_2O elimination, and including electron correlation improves the agreement. In particular, DFT predictions for activation energies for HF and H_2O elimination reactions are within 1 kcal mol^{-1} of the experimental values.

I. Introduction

Recently, 2-fluoroethanol (FEOH) has been suggested as a replacement for chlorofluorocarbons (CFC).[1] It is important to know all of the physical and chemical properties of molecules that are being considered for such applications before they are put into commercial use. Often incineration is the method of choice for disposing of used chemicals, and experimental data on the mechanism of pyrolysis would be valuable. However, there are no experimental or theoretical reports yet on the thermal decomposition of FEOH. Moreover, we have been interested in HX elimination reactions from haloethanes and recently reported our results on HCl elimination from 1,2-dichloroethane.[2] The substitution effect on the barrier to HX elimination from haloethanes has been studied in detail both experimentally[2−14] and theoretically.[15,16] However, the effect of OH substitution on HX elimination has rarely been addressed, except for one report on 2-chloroethanol.[14]

Thermal decomposition of ethanol has attracted much interest as well.[17−21] However, as is evident from a recent paper by Lin and co-workers,[22] there is still a need for reliable high-temperature kinetic data for ethanol. Both C−C dissociation and H_2O elimination channels are important for ethanol, and most of the thermal studies[17−21] showed the dominance of C−C dissociation. Chemical activation studies[23] and unpublished shock tube results from Lin and co-workers[22] have identified H_2O elimination as well. Halogen substitution on ethanol opens up the possibility for another low-barrier channel, namely, HX elimination, and indeed the report on CH_2Cl-CH_2OH has identified only the HCl elimination channel.[14] It would be interesting, as well, to study the effect of halogen substitution on the barrier to H_2O elimination. With these considerations, we have initiated studies on thermal decomposition of haloethanols in a single pulse shock tube, and this manuscript reports our results on 2-fluoroethanol. A future publication will address in detail the thermal decompositions of 2-chloroethanol and ethanol.

There have been numerous reports, both theoretical and experimental, on FEOH recently.[24−31] All of these reports have considered the structure, vibrational frequencies, isomerization, and intramolecular vibrational energy redistribution (IVR) of the ground state and rotational isomers. In this manuscript, we discuss the high-barrier HF and H_2O elimination reactions from FEOH. Single pulse shock tube and ab initio and DFT methods have been used to study the thermal decomposition of FEOH between 1000 and 1200 K. Theoretical studies have been carried out to characterize the transition state (TS) for both reactions. Transition-state theory (TST) calculations using theoretical results have been performed for comparison with experimental results.

II. Materials and Methods

II.A. Experimental Details. The shock tube facility used in this study has been described in detail in an earlier publication[2], and only a brief summary is given here. It is an aluminum tube of 51 mm internal diameter and 25 mm wall thickness. The lengths of the driven section and driver section can be varied by attaching/detaching small segments of the tube. In these experiments, the length of the driver section was 1850 mm and that of the driven section was 2581 mm. The dwell time was

* To whom correspondence should be addressed. E-mail: arunan@ipc.iisc.ernet.in.
† Department of Inorganic and Physical Chemistry.
# Current Address: Aeronamy Laboratory, NOAA, Boulder, CO 80305.
‡ Department of Aerospace Engineering.

10.1021/jp027323x CCC: $25.00
Published on Web 10/24/2003

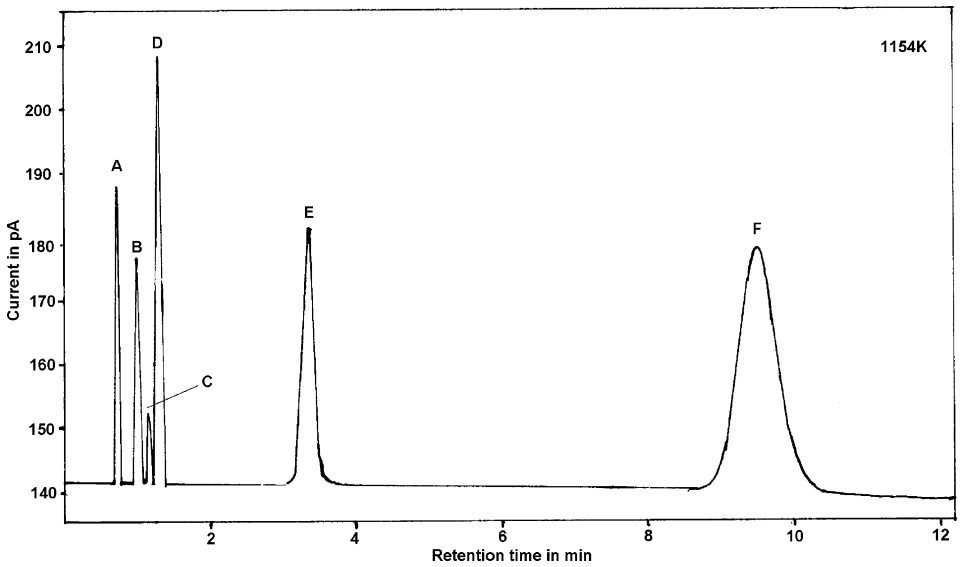

Figure 1. Gas chromatogram of a postshock mixture of 2-fluoroethanol in argon heated to 1154 K obtained on a 2-m Porapak Q column using FID: (A) methane; (B) ethylene; (C) ethane; (D) vinyl fluoride; (E) acetaldehyde; (F) 2-fluoroethanol.

typically 1200 μs. The experimental procedure is very similar to that suggested by Tsang for single pulse shock tube experiments.[13] A 1% mixture of 2-fluoroethanol in argon was prepared manometrically in a 10 L Pyrex glass bulb. This mixture was used in all of the runs. The shock tube was evacuated to 10^{-6} Torr before the experiment with a 6 in. diffusion pump. The ball valve was kept closed, and the FEOH mixture was loaded into the sample chamber (between the ball valve and the end flange) to 20−40 Torr using a mercury manometer. The sample was further diluted with argon until a desired pressure is reached. The final concentration of the sample was in the range of 500−1000 ppm. The segment of the driven section from the diaphragm to the ball valve was filled only with argon to a slightly larger pressure (4−6 Torr higher) than the sample chamber to avoid the back diffusion of the test gas. In all of the experiments, this pressure (P_1) was varied between 400 and 650 Torr. Just before rupturing the diaphragm, the ball valve was opened, and soon after the experiment, the ball valve was closed. The reaction dwell time was determined from the experimental pressure trace, and the reflected temperature was estimated using an external standard, that is, HCl elimination from ethyl chloride under similar conditions.[2]

II.B. Materials and Analysis. Spectroscopic grade 2-fluoroethanol (>99.5%, Lancaster chemicals Inc.) was used as received. For degassing and further purification, the freeze−pump−thaw method was used several times before making the sample. The purity of the reactant was routinely confirmed by gas chromatography. The postshock gas mixture was analyzed, quantitatively, by using an HP6890^{plus} gas chromatograph (GC) with flame ionization detector and, qualitatively, by IR spectrometer (Bruker Equinox 55 FTIR). The sample section of the shock tube was connected to the GC, and 0.5 mL of the mixture was injected through an online sampling valve. Porapak (6 ft length) Q column was found to be suitable for both the reactant and products. The major products formed in the process of thermal decomposition are CH_2═CHF and CH_3CHO. The other observed products were CH_4, C_2H_4, and C_2H_6. Some trace amounts of propylene were also formed at temperatures above 1150 K but were too small to be quantified. The GC analysis was carried out at a constant oven temperature (413 K). A typical chromatogram of the reaction mixture at the temperature, 1154 K, is shown in Figure 1. The initial concentration of reactant was obtained by summing up the concentrations of all of the species, except for ethane. Ethane concentration was multiplied by 2 because two FEOH are required to form ethane according to the kinetic mechanism that fits all experimental observation.

The sensitivity of the detector toward each compound was determined with standard samples: 2-fluoroethanol (Lancaster chemicals Inc.), acetaldehyde (Merck), ethyl chloride and vinyl fluoride (Fluka), ethylene (Hydrogas), and methane, ethane, and propylene (Bhoruka Gases). All of the other gases used in GC analysis such as argon, helium, oxygen, and hydrogen were from Bhoruka Gases, India (UHP grade 99.999%).

II.C. Computational Details. All calculations have been performed with the Gaussian 94 program suite.[32] Geometry optimizations have been carried out at Hartree−Fock (**HF**), second-order Møller−Plesset perturbation theory (MP2(FULL)), and density functional theory (DFT) levels with the standard 6-31G*, 6-31G**, 6-31+G**, and 6-311++G** basis sets that are internally available in the program suite. Equilibrium and transition-state structures were fully optimized using Hartree−Fock, second-order Møller−Plesset perturbation theory with all the electrons correlated, and the density functional theory with the B3LYP correlation functional. All transition states have been characterized with frequency analysis. Vibrational frequencies and zero-point energies were not scaled. These results were used in performing transition-state theory (TST) calculations to predict the activation energy and the preexponential factors for the HF and H_2O elimination reactions for comparison with experimental measurements. For additional comparison, calculations on H_2O elimination from ethanol were carried out as well, and the results are included. The enthalpy of formation of FEOH is not available to the best of our knowledge, and it was determined at the MP2/6-311++G** level. Our main interest in determining this quantity was to get a rough estimate of the internal energy in the products.

III. Experimental Results and Discussion

Thirty-four experiments were carried out between $T = 940$ and 1200 K, and postshock mixtures were quantitatively analyzed with GC. Details of the experimental conditions and the product distribution are given in the Table 1. It includes the temperature, T_5, the pressure, P_5, the dwell time, and concentrations of all the observed species. The P_5 was above

TABLE 1: Summary of the Experimental Results of 2-Fluoroethanol

no	T_5 (K)	P_5 (atm)	dwell time (μs)	$[CH_4]_t/[FEOH]_0$	$[C_2H_4]_t/[FEOH]_0$	$[C_2H_6]_t/[FEOH]_0$	$[C_2H_3F]_t/[FEOH]_0$	$[CH_3CHO]_t/[FEOH]_0$	$[FEOH]_t/[FEOH]_0$
1	936	13.2	1150	0	0	0	0	0.013 400	0.986 600
2	961	14.2	1210	0	0	0	0	0.002 050	0.997 950
3	963	13.9	1160	0	0	0	0	0.002 160	0.997 840
4	969	14.2	1140	0.000 240	0	0	0	0.001 700	0.998 060
5	983	15.0	1230	0.003 500	0	0	0	0.006 160	0.990 340
6	986	15.0	1200	0.000 260	0	0	0	0.003 250	0.996 490
7	986	15.1	1220	0.000 168	0	0	0	0.002 330	0.997 500
8	987	15.2	1160	0.000 127	0	0	0	0.002 210	0.997 670
9	1009	16.6	1380	0.000 155	0	0	0	0.002 970	0.996 870
10	1013	15.8	1180	0.003 940	0	0	0	0.007 200	0.988 860
11	1014	16.2	1240	0.000 141	0	0	0.000 201	0.004 100	0.995 560
12	1018	16.6	1240	0.000 212	0	0	0.000 113	0.003 500	0.996 170
13	1028	16.7	1240	0.000 286	0	0	0.000 326	0.006 270	0.993 120
14	1033	16.9	1230	0.000 345	0	0	0.000 246	0.006 270	0.993 140
15	1055	17.8	1230	0.000 444	0.000 311	0	0.000 645	0.009 230	0.989 360
16	1055	17.7	1240	0.000 043	0.000 211	0	0.000 644	0.007 610	0.991 100
17	1056	18.0	1230	0.000 471	0.000 366	0	0.000 707	0.008 560	0.989 900
18	1062	18.1	1260	0.000 582	0.000 517	0	0.001 030	0.009 370	0.988 490
19	1064	17.7	1230	0.000 698	0.000 737	0	0.001 190	0.011 660	0.985 720
20	1067	17.8	1230	0.006 140	0.003 880	0	0.009 500	0.041 510	0.938 980
21	1078	18.4	1220	0.001 010	0.000 765	0	0.001 680	0.014 370	0.982 170
22	1098	19.3	1200	0.001 960	0.001 950	0.000 360	0.004 140	0.028 050	0.963 530
23	1099	19.3	1140	0.002 430	0.002 410	0.000 501	0.005 180	0.034 210	0.955 260
24	1115	20.0	1200	0.002 620	0.002 840	0.000 381	0.005 230	0.033 950	0.954 980
25	1119	20.3	1180	0.002 880	0.002 830	0.000 569	0.005 860	0.035 120	0.952 730
26	1123	20.2	1200	0.005 800	0.008 560	0.001 730	0.010 940	0.068 820	0.904 160
27	1126	20.3	1210	0.004 690	0.008 170	0.001 370	0.009 170	0.059 060	0.917 530
28	1136	20.4	1310	0.007 190	0.008 610	0.001 690	0.014 050	0.073 550	0.894 910
29	1146	20.9	1210	0.007 32	0.010 320	0.002 210	0.013 100	0.075 160	0.891 890
30	1154	21.4	1200	0.007 43	0.010 400	0.002 360	0.013 570	0.077 080	0.889 150
31	1166	22.3	1280	0.010 6	0.014 860	0.003 460	0.018 820	0.098 830	0.853 420
32	1176	22.3	1160	0.017 02	0.023 660	0.005 850	0.027 090	0.132 180	0.794 190
33	1186	23.0	1270	0.023 95	0.034 740	0.009 630	0.031 020	0.162 100	0.738 550
34	1196	23.4	1260	0.031 75	0.044 110	0.013 350	0.034 010	0.152 720	0.724 060

13 atm in all runs, and our analysis assumed that the FEOH unimolecular reactions are in the first-order limit. In addition to the products listed in Table 1, CO was identified by using the infrared spectrum of the postshock gas mixture but was not quantified. Acetaldehyde was observed at all T in our study, whereas methane was observed only above 970 K. Ethylene and ethane are found to be products above 1050 and 1100 K, respectively. Vinyl fluoride is observed above 1015 K. The concentrations of ethane, ethylene, and methane are significant only at higher temperatures, that is, above 1150 K. Less than 28% of the reactants are consumed within the temperature range and dwell times of our experiments. Figure 2 shows the Arrhenius plot of the rate constant for overall decomposition of FEOH calculated as follows:

$$k_{\text{total}} = -\ln\{[\text{FEOH}]_t/[\text{FEOH}]_0\}/t \qquad (1)$$

The result is $k_{\text{total}} = 10^{13.55\pm0.32}\exp[-(60.6 \pm 1.6)/(RT)]\ \text{s}^{-1}$, where E_a is given in kcal mol^{-1}. $[\text{FEOH}]_t$ and $[\text{FEOH}]_0$ are the experimentally measured concentration of FEOH at the end of the reaction time t and initial concentration, respectively. This plot is linear within the temperature range of analysis (1000−1200 K) and suggests that the overall decomposition of 2-fluoroethanol is unimolecular. In the case of nitromethane, Zhang and Bauer[33] noted curvature in the Arrhenius plot, which was attributed to the consumption of nitromethane by secondary reaction with radicals. From the Arrhenius plot given in Figure 2, it appears that the FEOH consumption under our experimental conditions is unaffected by secondary reactions.

III.A. Major Channels. The major channels through which 2-fluoroethanol decomposes are unimolecular elimination

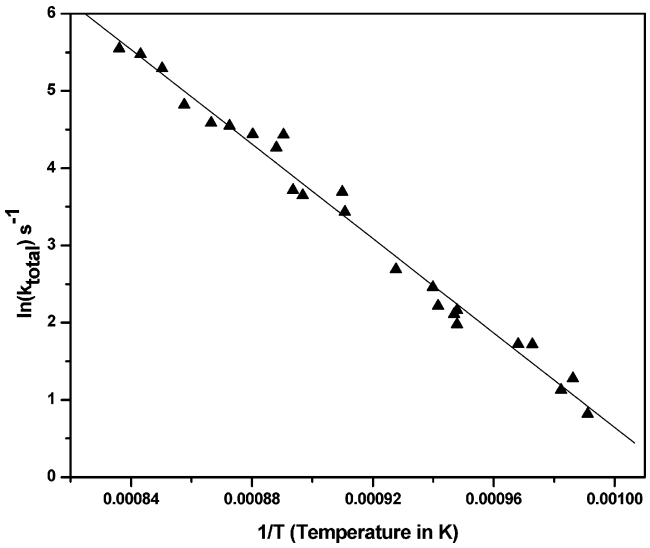

Figure 2. Arrhenius plot for the overall decomposition of 2-fluoroethanol.

of HF and H_2O:

$$\text{F}-\text{CH}_2\text{CH}_2-\text{OH} \rightarrow \text{HF} + \text{CH}_2{=}\text{CH}-\text{OH} \qquad (\text{R1})$$

$$\text{F}-\text{CH}_2\text{CH}_2-\text{OH} \rightarrow \text{H}_2\text{O} + \text{CH}_2{=}\text{CH}-\text{F} \qquad (\text{R2})$$

(The reaction numbers here and throughout the text correspond to the list in Table 2, which gives the complete mechanism used for simulating the profiles of all products). The vinyl alcohol formed in reaction R1 presumably isomerizes to acetaldehyde,

TABLE 2: The Reaction Scheme Proposed for the Thermal Decomposition of 2-Fluoroethanol[a]

reaction number	reaction	rate expression	reference
R1	$F-CH_2-CH_2-OH \rightarrow CH_3CHO + HF$	$k_1 = 1.507 \times 10^{13} \exp[-59\,456/(RT)]\ s^{-1}$	this work
R2	$F-CH_2-CH_2-OH \rightarrow CH_2{=}CH-F + H_2O$	$k_2 = 2.0067 \times 10^{14} \exp[-69\,690/(RT)]\ s^{-1}$	this work
R3	$CH_2{=}CH-F \rightarrow CH{\equiv}CH + HF$	$k_3 = 2.398 \times 10^{14} \exp[-81\,400/(RT)]\ s^{-1}$	39
R4	$CH_3CHO \rightarrow CH_3 + CHO$	$k_4 = 1.21 \times 10^{13} \exp[-57\,200/(RT)]\ s^{-1}$	38
R5	$CH_3CHO \rightarrow CH_4 + CO$	$k_5 = 1.21 \times 10^{12} \exp[-57\,200/(RT)]\ s^{-1}$	38
R6	$CHO \rightarrow CO + H$	$k_6 = 5.11 \times 10^{21}(T)^{-2.14} \exp[-20\,425/(RT)]\ s^{-1}$	53
R7	$CHO + H \rightarrow CO + H_2$	$k_7 = 1.2 \times 10^{14}\ cm^3\ mol^{-1}\ s^{-1}$	53
R8	$CH_3 + CHO \rightarrow CH_3CHO$	$k_8 = 1.8129 \times 10^{13}\ cm^3\ mol^{-1}\ s^{-1}$	54
R9	$CH_3 + CH_3CHO \rightarrow CH_4 + CH_3CO$	$k_9 = 1.98 \times 10^{-6}(T)^{5.64} \exp[-2464/(RT)]\ cm^3\ mol^{-1}\ s^{-1}$	55
R10	$CH_3 + CH_3CHO \rightarrow CH_4 + CH_2CHO$	$k_{10} = 4.5 \times 10^{-1}(T)^{4.0} \exp[-8280/(RT)]\ cm^3\ mol^{-1}\ s^{-1}$	34
R11	$H + CH_3CHO \rightarrow H_2 + CH_2CHO$	$k_{11} = 2.4 \times 10^{1}(T)^{3.5} \exp[-5167/(RT)]\ cm^3\ mol^{-1}\ s^{-1}$	53
R12	$H + CH_3CHO \rightarrow H_2 + CH_3CO$	$k_{12} = 8.7 \times 10^{13} \exp[-4200/(RT)]\ cm^3\ mol^{-1}\ s^{-1}$	34
R13	$CH_2CHO \rightarrow H + CH_2CO$	$k_{13} = 1.58 \times 10^{13} \exp[-34\,974/(RT)]\ s^{-1}$	56
R14	$CH_3CO \rightarrow CH_3 + CO$	$k_{14} = 8.73 \times 10^{42}(T)^{-8.62} \exp[-22\,455/(RT)]\ s^{-1}$	54
R15[a]	$CH_3 + CH_3 \rightarrow C_2H_6$	$k_{15} = 6.8 \times 10^{14}(T)^{-0.64}\ cm^3\ mol^{-1}\ s^{-1}$	53
R16[a]	$CH_3 + CH_3 \rightarrow C_2H_4 + H_2$	$k_{16} = 9.9 \times 10^{15} \exp[-32\,987/(RT)]\ cm^3\ mol^{-1}\ s^{-1}$	57
R17[a]	$CH_3 + CH_3 \rightarrow C_2H_5 + H$	$k_{17} = 2.4 \times 10^{13} \exp[-12\,877/(RT)]\ cm^3\ mol^{-1}\ s^{-1}$	58
R18	$CH_3 + C_2H_6 \rightarrow CH_4 + C_2H_5$	$k_{18} = 0.548(T)^{4.0} \exp[-8285/(RT)]\ cm^3\ mol^{-1}\ s^{-1}$	53
R19	$H + C_2H_6 \rightarrow C_2H_5 + H_2$	$k_{19} = 5.54 \times 10^{2}(T)^{3.5} \exp[-5167/(RT)]\ cm^3\ mol^{-1}\ s^{-1}$	53
R20	$C_2H_5 \rightarrow C_2H_4 + H$	$k_{20} = 4.8 \times 10^{8}(T)^{1.19} \exp[-37\,205/(RT)]\ s^{-1}$	53
R21	$C_2H_5 + H \rightarrow C_2H_4 + H_2$	$k_{21} = 1.81 \times 10^{12}\ cm^3\ mol^{-1}\ s^{-1}$	53
R22	$C_2H_5 + H \rightarrow C_2H_6$	$k_{22} = 4.86 \times 10^{12}\ cm^3\ mol^{-1}\ s^{-1}$	53
R23	$C_2H_5 + C_2H_5 \rightarrow C_2H_4 + C_2H_6$	$k_{23} = 1.39 \times 10^{12}\ cm^3\ mol^{-1}\ s^{-1}$	54
R24	$C_2H_5 + C_2H_5 \rightarrow C_4H_{10}$	$k_{24} = 1.078 \times 10^{13}\ cm^3\ mol^{-1}\ s^{-1}$	54
R25	$C_2H_5 + H \rightarrow CH_3 + CH_3$	$k_{25} = 1.68 \times 10^{13}\ cm^3\ mol^{-1}\ s^{-1}$	53
R26	$C_2H_5 + CH_3 \rightarrow C_2H_4 + CH_4$	$k_{26} = 9.8 \times 10^{12}(T)^{-0.5}\ cm^3\ mol^{-1}\ s^{-1}$	53
R27	$C_2H_5 + CH_3 \rightarrow C_4H_8$	$k_{27} = 2.45 \times 10^{14}(T)^{-0.5}\ cm^3\ mol^{-1}\ s^{-1}$	53
R28	$C_2H_5 + CHO \rightarrow C_2H_6 + CO$	$k_{28} = 1.2 \times 10^{14}\ cm^3\ mol^{-1}\ s^{-1}$	53
R29	$C_2H_5 + CH_3CHO \rightarrow C_2H_6 + CH_3CO$	$k_{29} = 2.25(T)^{3.65} \exp[-9141/(RT)]\ cm^3\ mol^{-1}\ s^{-1}$	53
R30	$C_2H_4 \rightarrow C_2H_2 + H_2$	$k_{30} = 7.94 \times 10^{12}(T)^{0.44} \exp[-88\,769/(RT)]\ s^{-1}$	54
R31	$C_2H_4 \rightarrow C_2H_3 + H$	$k_{31} = 2.58 \times 10^{17} \exp[-96\,578/(RT)]\ s^{-1}$	55
R32	$C_2H_4 + CH_3 \rightarrow C_3H_6 + H$	$k_{32} = 2.0 \times 10^{13} \exp[-10\,000/(RT)]\ cm^3\ mol^{-1}\ s^{-1}$	53
R33	$C_2H_4 + CH_3 \rightarrow C_2H_3 + CH_4$	$k_{33} = 6.62(T)^{3.7} \exp[-9499/(RT)]\ cm^3\ mol^{-1}\ s^{-1}$	53
R34	$C_2H_4 + H \rightarrow C_2H_3 + H_2$	$k_{34} = 1.32 \times 10^{6}(T)^{2.53} \exp[-12\,241/(RT)]\ cm^3\ mol^{-1}\ s^{-1}$	54
R35	$C_2H_4 + C_2H_5 \rightarrow C_2H_6 + C_2H_3$	$k_{35} = 6.32 \times 10^{2}(T)^{3.13} \exp[-18\,011/(RT)]\ cm^3\ mol^{-1}\ s^{-1}$	53
R36	$C_2H_3 \rightarrow C_2H_2 + H$	$k_{36} = 4.1 \times 10^{41}(T)^{-7.49} \exp[-45\,506/(RT)]\ s^{-1}$	54
R37	$C_2H_3 + H \rightarrow C_2H_2 + H_2$	$k_{37} = 9.6 \times 10^{13}\ cm^3\ mol^{-1}\ s^{-1}$	54
R38[a]	$CH_4 \rightarrow CH_3 + H$	$k_{38} = 7.8 \times 10^{14} \exp[-103\,826/(RT)]\ s^{-1}$	53
R39[a]	$CH_4 + H \rightarrow CH_3 + H_2$	$k_{39} = 2.244 \times 10^{4}(T)^{3} \exp[-8763/(RT)]\ cm^3\ mol^{-1}\ s^{-1}$	54
R40	$CH_2CO \rightarrow CH_2 + CO$	$k_{40} = 3.0 \times 10^{14} \exp[-70\,943/(RT)]\ s^{-1}$	59
R41[a]	$CH_2CO + H \rightarrow CH_3 + CO$	$k_{41} = 1.8 \times 10^{13}\ cm^3\ mol^{-1}\ s^{-1}$	60
R42	$CH_2 + CH_2 \rightarrow C_2H_2 + H_2$	$k_{42} = 2.99 \times 10^{13}\ cm^3\ mol^{-1}\ s^{-1}$	61
R43	$CH_3 + CH_2 \rightarrow C_2H_4 + H$	$k_{43} = 4.2221 \times 10^{13}\ cm^3\ mol^{-1}\ s^{-1}$	55
R44	$CH_3 + CHO \rightarrow CH_4 + CO$	$k_{44} = 1.21 \times 10^{14}\ cm^3\ mol^{-1}\ s^{-1}$	54
R45	$CH_2 + CH_2 \rightarrow C_2H_4$	$k_{45} = 1.0 \times 10^{12}\ cm^3\ mol^{-1}\ s^{-1}$	62
R46[b]	$F-CH_2-CH_2-OH \rightarrow HOF + C_2H_4$	$k_{46} = 2.01 \times 10^{17} \exp[-85\,929/(RT)]\ s^{-1}$	this work
R47	$CH_2 + CH_2CO \rightarrow C_2H_4 + CO$	$k_{47} = 3.981 \times 10^{13} \exp[-8365.2/(RT)]\ cm^3\ mol^{-1}\ s^{-1}$	62
R48	$C_2H_3 + CHO \rightarrow C_2H_4 + CO$	$k_{48} = 9.05 \times 10^{13}\ cm^3\ mol^{-1}\ s^{-1}$	54
R49	$CH_3 + FC_2H_4OH \rightarrow CH_4 + FCHCH_2OH$	$k_{49} = 3.98 \times 10^{11} \exp[-9697.7/(RT)]\ cm^3\ mol^{-1}\ s^{-1}$	40
R50	$C_2H_5 + FC_2H_4OH \rightarrow CH_4 + FCHCH_2OH$	$k_{50} = 3.98 \times 10^{11} \exp[-9697.7/(RT)]\ cm^3\ mol^{-1}\ s^{-1}$	40
R51	$FCHCH_2OH \rightarrow CH_2{=}CHF + OH$	$k_{51} = 6.19 \times 10^{11} \exp[-23\,647/(RT)]\ s^{-1}$	63
R52	$CH_3 + OH \rightarrow CH_3OH$	$k_{52} = 6.023 \times 10^{13}\ cm^3\ mol^{-1}\ s^{-1}$	54
R53	$C_2H_5 + OH \rightarrow C_2H_5OH$	$k_{53} = 7.709 \times 10^{13}\ cm^3\ mol^{-1}\ s^{-1}$	64
R54[b]	$FCH_2CH_2OH \rightarrow FCH_2CH_2 + OH$	$k_{54} = 2.01 \times 10^{17} \exp[-86\,095/(RT)]s^{-1}$	this work
R55	$FCH_2CH_2 \rightarrow C_2H_4 + F$	$k_{55} = 3.90 \times 10^{13} \exp[-21\,660/(RT)]s^{-1}$	65
R56	$OH + FCH_2CH_2OH \rightarrow H_2O + FCH_2CHOH$	$k_{56} = 3.98 \times 10^{11} \exp[-9697.7/(RT)]\ cm^3\ mol^{-1}\ s^{-1}$	40
R57	$OH + FCH_2CH_2OH \rightarrow H_2O + FCHCH_2OH$	$k_{57} = 3.98 \times 10^{11} \exp[-13\,697.7/(RT)]\ cm^3\ mol^{-1}\ s^{-1}$	40
R58	$F + FCH_2CH_2OH \rightarrow HF + FCH_2CHOH$	$k_{58} = 3.98 \times 10^{11} \exp[-9697.7/(RT)]\ cm^3\ mol^{-1}\ s^{-1}$	40
R59	$F + FCH_2CH_2OH \rightarrow HF + FCHCH_2OH$	$k_{59} = 3.98 \times 10^{11} \exp[-13\,697.7/(RT)]\ cm^3\ mol^{-1}\ s^{-1}$	40
R60	$O + FCH_2CH_2OH \rightarrow HO + FCH_2CHOH$	$k_{60} = 3.98 \times 10^{11} \exp[-9697.7/(RT)]\ cm^3\ mol^{-1}\ s^{-1}$	40
R61	$O + FCH_2CH_2OH \rightarrow HO + FCHCH_2OH$	$k_{61} = 3.98 \times 10^{11} \exp[-13\,697.7/(RT)]\ cm^3\ mol^{-1}\ s^{-1}$	40
R62	$F + OH \rightarrow HF + O$	$k_{62} = 5.902 \times 10^{12} \exp[-5683.3/(RT)]\ cm^3\ mol^{-1}\ s^{-1}$	66
R63	$HF + O \rightarrow OH + F$	$k_{63} = 1.210 \times 10^{10}\ cm^3\ mol^{-1}\ s^{-1}$	66
R64	$O + O + Ar \rightarrow O_2 + Ar$	$k_{64} = 2.74 \times 10^{13} \exp[-0.971/(RT)]\ cm^6 mol^{-2}\ s^{-1}$	67
R65	$F + F + Ar \rightarrow F_2 + Ar$	$k_{65} = 1.00 \times 10^{14}\ cm^6\ mol^{-2}\ s^{-1}$	68
R66	$FCH_2CHOH \rightarrow F + CH_3CHO$	$k_{66} = 6.19 \times 10^{11} \exp[-23\,647/(RT)]\ s^{-1}$	63

[a] For reactions R15, R17, R25, R38, R39, and R41 revised rate constants are available. Reactions R16, R21, and R22 are negligible (refs 69−74). See note added at the end of section III in text. [b] Reactions R54 and R55 can replace reaction R46 to explain the ethylene formation equally well. Reactions R56−R66 are added to account for the radical reactions that are likely as the result of reactions R54 and R55. With our experimental results, the two options, that is, direct HOF elimination [reaction R46] or successive bond dissociation [reactions R54 and R55], cannot be distinguished.

which has been observed. Water elimination leads to the formation of vinyl fluoride. By monitoring the concentrations of C_2H_3F and CH_3CHO at various temperatures, it is possible to extract the rate constants for the H_2O and HF elimination reactions. However, the CH_3CHO is consumed by secondary reactions, as is evident from the formation of CH_4, even at lower temperatures. Hence, first the concentration of C_2H_3F was followed to estimate the rate constant for H_2O elimination, and Figure 3a shows the Arrhenius plot. The rate constant for the dominant HF elimination channel was then estimated by monitoring the FEOH and CH_3CHO. It involved kinetic simulation with fewer steps and data points, and Figure 3b gives the Arrhenius plot for this reaction. A detailed kinetic simulation of all of the major and minor products and comparisons with their experimentally observed profiles further refined and confirmed these rate constants.

III.B. Minor Channels and Secondary Reactions. Methane has been observed along with acetaldehyde, and it is most likely formed by acetaldehyde decomposition. The FEOH cannot lead to methane either directly or through any other simple radical processes. Direct studies on the thermal decomposition of acetaldehyde[34] in reflected shock waves in the temperature range of 1400−1800 K reveal that the primary step in the decomposition process is C−C bond dissociation; the activation energy for the process is 81.9 kcal mol^{-1}.

$$CH_3CHO \rightarrow CH_3 + CHO$$
$$k = 7.08 \times 10^{15} \exp[-81\,872/(RT)]\ s^{-1} \quad \text{(R4)}$$

The rate constant for this reaction at 970 K, at which temperature CH_4 has been noted, is 0.002 s^{-1}. Hence, its contribution to the formation of methyl radicals and CH_4 is negligible. Also, the fact that C_2H_6 has not been observed until $T > 1100$ K suggests that CH_3 radicals are not present in significant concentrations below this temperature. Direct CH_4 formation from CH_3CHO has been considered, and it is a high-barrier (>80 kcal mol^{-1}) process as well.[35]

$$CH_3CHO \rightarrow CH_4 + CO \quad \text{(R5)}$$

Because the preexponential factor for this molecular elimination process should be significantly smaller than that of reaction R4, this reaction is unlikely. However, CH_3CHO that is produced by the isomerization of CH_2═CHOH is "chemically active", and the effective barriers for reactions R4 and R5 may be less. The enthalpy of formation[36] for CH_3CHO (−39.7 kcal mol^{-1}) is 10 kcal mol^{-1} less than that of CH_2═CHOH (−29.8 kcal mol^{-1}). However, the barrier for isomerization[37] is estimated to be 55 kcal mol^{-1}. The enthalpy of formation for FEOH is not available to the best of our knowledge. From our MP2/6-311++G** calculations, it is determined to be −109.4 kcal mol^{-1}. At this level, the FEOH → CH_3CHO + HF reaction is 6 kcal mol^{-1} exoergic. Considering the fact that the activation energy for HF elimination from FEOH is determined to be 60 kcal mol^{-1} in this work, it is clear that most of the available energy from the HF elimination reaction will remain as internal energy in the polyatomic product. Lifshtiz and Ben-Hamou reported the thermal decomposition of ethylene oxide,[38] the first step of which was found to be isomerization to give chemically active acetaldehyde. Coincidentally, they have observed the same side products, namely, CH_4, C_2H_4, and C_2H_6. Considering the fact that CH_3CHO was chemically active, they used lower barriers for both reactions R4 and R5 to account for the formation of these products in the lower-temperature range.

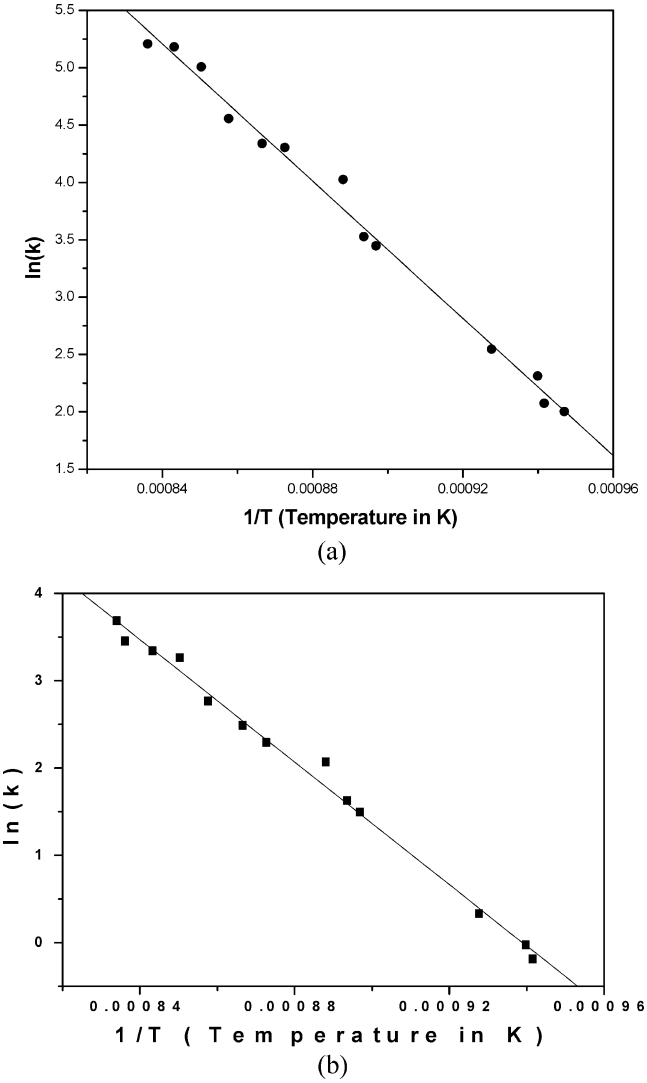

Figure 3. Arrhenius plot for the unimolecular elimination of (a) hydrogen fluoride and (b) H_2O from 2-fluoroethanol (k is in s^{-1}).

Vinyl fluoride decomposition behind the reflected shock waves has also been reported,[39] and the activation energy is nearly the same as that for acetaldehyde decomposition. Unimolecular elimination of HF is the major channel through which it decomposes to give acetylene.

$$CH_2{=}CHF \rightarrow C_2H_2 + HF$$
$$k_3 = 2.398 \times 10^{14} \exp[-81\,400/(RT)] \quad \text{(R3)}$$

Even at the higher temperature range of this present study, the rate constant for this reaction is 0.3 s^{-1}. Hence, the contribution of reaction R3 toward the formation of acetylene is expected to be negligible. Acetylene was not observed in our experiments at all, and this confirms that, within our experimental conditions, these high-barrier reactions are not contributing. Evidently, vinyl fluoride, which is directly formed through reaction R2, is not "chemically active".

To account for the formation of these products, a detailed kinetic simulation was carried out. In addition to reactions R1 and R2, the acetaldehyde pyrolysis steps were included.[38] A reaction scheme containing 27 species and 53 reactions for the decomposition of 2-fluoroethanol was used for the simulation. Table 2 contains all of the proposed reactions and their rate expressions, along with the references. The scheme is composed

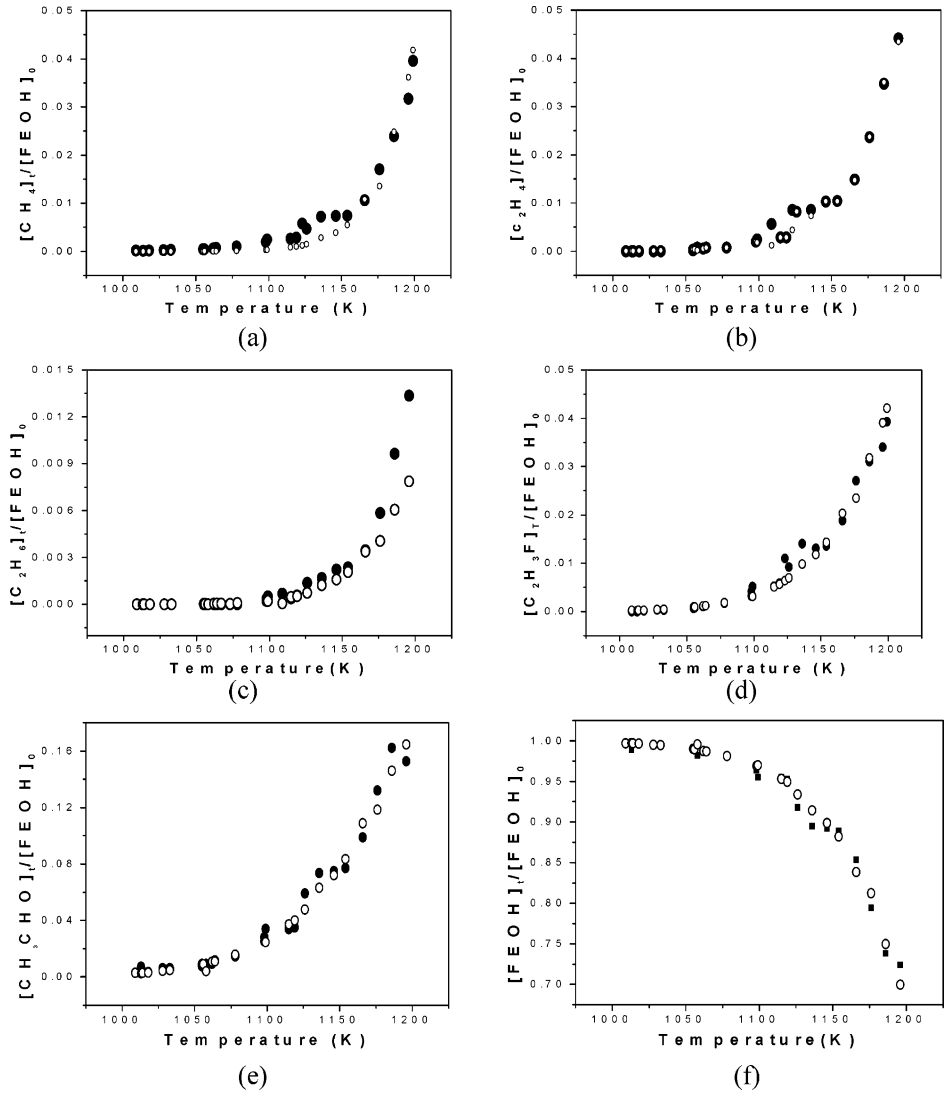

Figure 4. Comparison between the experimental and calculated concentrations of (a) methane, (b) ethylene, (c) ethane, (d) vinyl fluoride, (e) acetaldehyde, and (f) 2-fluoroethane. Filled circles on the plot are the experimental concentrations, and the open circles are simulated concentrations.

of unimolecular dissociation of the reactant molecule, unimolecular dissociation of the radical intermediates, abstraction, and recombination reactions. The rate constants were varied within the limits of the reported uncertainties. The rate expressions for reactions R1, R2, and R46 (vide infra) were evaluated from our experimental results. The simulation was carried out for the dwell time, and not surprisingly, all of the radicals were not consumed within this time. The kinetic simulation was extended for a few more milliseconds, but the rate constants were evaluated at room temperature (298 K). We note again that Zhang and Bauer have used a similar approach to model nitromethane decomposition.[33] Consumption of FEOH by reactions with radicals, reactions R49 and R50, was included, but it was found that these reactions did not play a significant role. Simulation was carried for 20 ms, and it was noted that the radicals were nearly completely consumed. The concentration profiles for all of the products were compared to the experimental results. Figure 4a−f shows the comparisons between the concentrations of products based on analyses of post-shock mixtures and those from kinetic simulation with the reaction scheme given in Table 2. The solid symbols in the figure are experimental points, and the open symbols show the simulated values. The agreement between the experimental concentrations and the simulated values is reasonable. All of the steps that lead to methane, ethane, and ethylene are discussed below.

1. Methane. Methane is formed directly from excited acetaldehyde by either direct molecular elimination or by C−C dissociation followed by the reaction between CH_3 and HCO:

$$CH_3CHO \rightarrow CH_3 + HCO$$
$$k_4 = 1.21 \times 10^{13} \exp[-57\,200/(RT)]\ s^{-1} \quad \text{(R4)}$$

$$CH_3CHO \rightarrow CH_4 + CO$$
$$k_5 = 1.21 \times 10^{12} \exp[-57\,200/(RT)]\ s^{-1} \quad \text{(R5)}$$

$$CH_3 + HCO \rightarrow CH_4 + CO$$
$$k_{44} = 1.21 \times 10^{14}\ cm^3\ mol^{-1}\ s^{-1} \quad \text{(R44)}$$

The reaction R44 competes with stabilization to CH_3CHO [reaction R8] and also CH_3 radical recombination [reaction R15]. Some other reactions were considered in the reaction scheme for the formation of CH_4:

$$CH_3 + C_2H_6 \rightarrow CH_4 + C_2H_5$$
$$k_{18} = 0.548(T)^{4.0} \exp[-8285/(RT)]\ \text{cm}^3\ \text{mol}^{-1}\ \text{s}^{-1} \quad \text{(R18)}$$

$$C_2H_5 + CH_3 \rightarrow C_2H_4 + CH_4$$
$$k_{26} = 9.8 \times 10^{12}(T)^{-0.5}\ \text{cm}^3\ \text{mol}^{-1}\ \text{s}^{-1} \quad \text{(R26)}$$

The contribution of these two reactions depends on the concentration of the ethane, as well as methyl radicals. Contributions from both of these reactions are small, but they were included for completeness because both ethane and ethyl are formed in subsequent steps.

The reaction of CH_3 with FEOH was considered because the reactant is present in large concentrations. The rate constant for this reaction is not available in the literature, and the rate constant for hydrogen abstraction reaction from ethanol was therefore used [reaction R49]. It was found that the FEOH consumption was insignificant. For the $CH_3 + CH_3CH_2OH$ reaction, it appears that only H abstraction mechanism has been considered.[40] Both in ethanol and in FEOH, the C−O bond (∼90 kcal mol^{-1}) is weaker than the C−H bonds (∼90−100 kcal mol^{-1}).[41] It appears that abstraction of OH could be important in these reactions, but we are not aware of any reports considering this possibility. In our experiments, methanol was not observed, and it is likely that CH_3 + FEOH reaction does not contribute significantly.

Reaction of CH_3 with CH_3CHO and subsequent reactions are included for completeness, and their contribution to CH_4 formation is very small. The consumption of the methane formed in the reaction scheme is taken into account in the following reactions.

$$CH_4 \rightarrow CH_3 + H$$
$$k_{38} = 7.8 \times 10^{14} \exp[-103\,826/(RT)]\ \text{s}^{-1} \quad \text{(R38)}$$

$$CH_4 + H \rightarrow CH_3 + H_2$$
$$k_{39} = 2.244 \times 10^4(T)^3 \exp[-8763/(RT)]\ \text{cm}^3\ \text{mol}^{-1}\ \text{s}^{-1} \quad \text{(R39)}$$

Reaction R38 has very high activation energy, and it is very unlikely in the present experimental conditions.

2. Ethane. The only major channel for the formation of ethane is the recombination of methyl radicals. The following reactions are included in the reaction scheme that can contribute to the production of ethane.

$$CH_3 + CH_3 \rightarrow C_2H_6$$
$$k_{15} = 6.8 \times 10^{14}(T)^{-0.64}\ \text{cm}^3\ \text{mol}^{-1}\ \text{s}^{-1} \quad \text{(R15)}$$

$$C_2H_5 + H \rightarrow C_2H_6 \qquad k_{22} = 4.86 \times 10^{12}\ \text{cm}^3\ \text{mol}^{-1}\ \text{s}^{-1} \quad \text{(R22)}$$

$$C_2H_5 + C_2H_5 \rightarrow C_2H_4 + C_2H_6$$
$$k_{23} = 1.39 \times 10^{12}\ \text{cm}^3\ \text{mol}^{-1}\ \text{s}^{-1} \quad \text{(R23)}$$

$$C_2H_5 + CHO \rightarrow C_2H_6 + CO$$
$$k_{28} = 1.2 \times 10^{14}\ \text{cm}^3\ \text{mol}^{-1}\ \text{s}^{-1} \quad \text{(R28)}$$

$$C_2H_4 + C_2H_5 \rightarrow C_2H_6 + C_2H_3$$
$$k_{35} = 6.32 \times 10^2(T)^{3.13} \exp[-18\,011/(RT)]\ \text{cm}^3\ \text{mol}^{-1}\ \text{s}^{-1} \quad \text{(R35)}$$

Though the reaction steps R22, R23, R28, and R35 form ethane, their contribution toward the formation of ethane is negligible because all of these reactions depend on the ethyl radical concentration, which is low. Reactions R18 and R19 are included in the scheme in which ethane is consumed.

3. Ethylene. Among all of the other products, ethylene concentration is the highest. About 4% of ethylene is found at the highest temperature. Initially it was assumed that ethylene could be the product from reactions of methyl and other radical products. Hence the following reactions were included in the scheme.

$$CH_3 + CH_3 \rightarrow C_2H_4 + H_2$$
$$k_{16} = 9.9 \times 10^{15} \exp[-32\,987/(RT)]\ \text{cm}^3\ \text{mol}^{-1}\ \text{s}^{-1} \quad \text{(R16)}$$

$$CH_3 + CH_3 \rightarrow C_2H_5 + H$$
$$k_{17} = 2.4 \times 10^{13} \exp[-12\,877/(RT)]\ \text{cm}^3\ \text{mol}^{-1}\ \text{s}^{-1} \quad \text{(R17)}$$

$$C_2H_5 \rightarrow C_2H_4 + H$$
$$k_{20} = 4.8 \times 10^8(T)^{1.19} \exp[-37\,205/(RT)]\ \text{s}^{-1} \quad \text{(R20)}$$

$$C_2H_5 + H \rightarrow C_2H_4 + H_2$$
$$k_{21} = 1.81 \times 10^{12}\ \text{cm}^3\ \text{mol}^{-1}\ \text{s}^{-1} \quad \text{(R21)}$$

$$C_2H_5 + C_2H_5 \rightarrow C_2H_4 + C_2H_6$$
$$k_{23} = 1.39 \times 10^{12}\ \text{cm}^3\ \text{mol}^{-1}\ \text{s}^{-1} \quad \text{(R23)}$$

$$C_2H_5 + CH_3 \rightarrow C_2H_4 + CH_4$$
$$k_{26} = 9.8 \times 10^{12}(T)^{-0.5}\ \text{cm}^3\ \text{mol}^{-1}\ \text{s}^{-1} \quad \text{(R26)}$$

All of these reactions involve methyl and ethyl radicals. Out of all of the above-mentioned reactions, reaction R16 is expected to contribute more because the methyl radical concentration is high when compared to ethyl and other radicals. However, it was found that the ethylene concentration predicted was much smaller than the experimental observation. The main reason is that the rate constant for reaction R15 (CH_3 recombination leading to ethane) is 2−3 orders of magnitude larger than that of reaction R16 or R17, which produce ethylene or ethyl radicals, respectively.

The CH_2 recombination to form ethylene is well-known. In our experiment, CH_2 can be formed through the following reaction scheme:

$$CH_3 + CH_3CHO \rightarrow CH_4 + CH_2CHO$$
$$k_{10} = 0.45T^{4.0} \exp[-8280/(RT)] \quad \text{(R10)}$$

$$CH_2CHO \rightarrow CH_2CO + H$$
$$k_{13} = 1.58 \times 10^{13} \exp[-34\,974/(RT)] \quad \text{(R13)}$$

$$CH_2CO \rightarrow CH_2 + CO$$
$$k_{40} = 3.0 \times 10^{14} \exp[-70\,943/(RT)] \quad \text{(R40)}$$

$$CH_2 + CH_2 \rightarrow C_2H_4 \qquad k_{45} = 1.0 \times 10^{12} \quad \text{(R45)}$$

However, even with all of these reactions, not even 10% of the total ethylene found experimentally could be accounted for. It appeared that there must be a direct reaction from FEOH producing ethylene. Klaassen et al.[42] have observed HOI

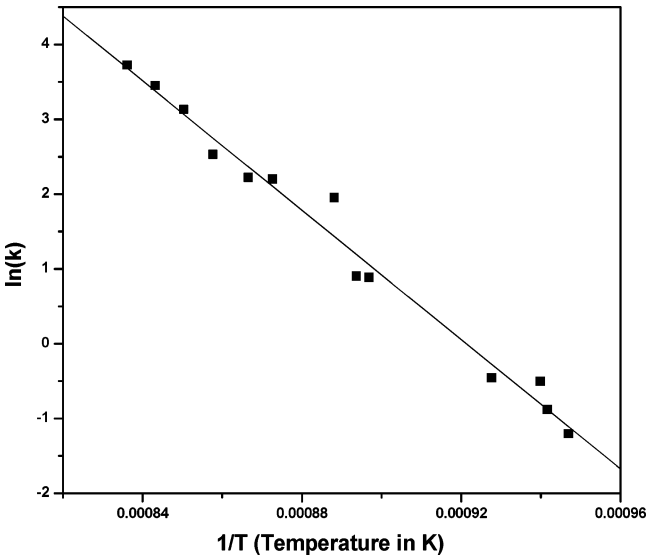

Figure 5. Arrhenius plot for the unimolecular elimination of HOF from 2-fluoroethanol (k is in s^{-1}).

formation from C_2H_5OI, which is obtained by reacting ethyl iodide with atomic oxygen (^3P). Leone and co-workers have reported recently[43] that HOI elimination competes with the elimination of HCl in the reaction of $O(^3P)$ with CH_2ICH_2Cl. This led us to consider the possibility of the unimolecular elimination of HOF from the reactant, that is, 2-fluoroethanol.

$$F-CH_2-CH_2-OH \rightarrow HOF + C_2H_4 \qquad \text{(R46)}$$

When this reaction was added in the scheme, the formation of ethylene in the thermal decomposition of 2-fluoroethanol could be explained quantitatively. The rate constant for this reaction was determined by simulation with fewer steps following FEOH, CH_3CHO, C_2H_3F, and C_2H_4. The Arrhenius plot for the unimolecular elimination of HOF from 2-fluoroethanol, which is obtained from the simulated fits, is shown in Figure 5. The rate constant for this process is determined to be $10^{17.30\pm0.66}$ $\exp[(-85.9 \pm 3.4)/(RT)]$ s^{-1}. The preexponential factor is significantly larger than HF or H_2O elimination. It is conceivable that both C−F and C−O bonds weaken, which could lead to several low-frequency stretching and bending modes at the TS. However, the activation energy of nearly 86 kcal mol^{-1} suggests that C−O bond dissociation reaction of FEOH cannot be ignored as a possible source of ethylene. Hence, the following steps were added instead of unimolecular elimination of HOF from FEOH to explain the formation of ethylene.

$$FCH_2CH_2OH \rightarrow FCH_2CH_2 + OH \qquad \text{(R54)}$$

$$FCH_2CH_2 \rightarrow CH_2CH_2 + F \qquad \text{(R55)}$$

The rate constant obtained for the C−O bond scission by fitting the concentration of C_2H_4 is $k_{54} = 10^{17.32\pm0.6}$ $\exp[(-86.1 \pm 2.3)/(RT)]s^{-1}$. Reaction R55 is fast under our conditions, and it will be difficult to distinguish between these two possibilities as source for C_2H_4. Not surprisingly, the fitted rate constants for reactions R46 and R54 are nearly the same. Reactions R56−R66 were also included in the mechanism to account for the radical consumptions. With these steps added, instead of the HOF elimination [reaction R46], the concentration profiles of all of the products could be simulated equally well. After addition of these steps, the rate constants for HF elimination and H_2O elimination are refined marginally, and they are $10^{13.1\pm0.3}$ $\exp[(-59.1 \pm 1.7)/(RT)]$ s^{-1} and $10^{14.6\pm0.4}$ $\exp[(-71.3 \pm 2.0)/(RT)]$ s^{-1}. Obviously, more experimental results are needed to verify the complete mechanism of pyrolysis.

4. Propylene. The only channel through which propylene can be formed using the present scheme is reaction R32].

$$C_2H_4 + CH_3 \rightarrow C_3H_6 + H$$
$$k_{32} = 2.0 \times 10^{13} \exp[-10\,000/(RT)]\ cm^3\ mol^{-1}\ s^{-1} \qquad \text{(R32)}$$

We could not quantify propylene in the experimental analysis because of its insignificant amounts. The present reaction scheme was also predicting very small amounts of propylene.

Note Added in Revision. Since completion of this work, it has been noted that rate constants for several steps, especially reactions R17, R25, R38, R39, and R41 have been refined. Sutherland, Su, and Michael[69] have reported direct measurements for reactions R38 and R39. For reaction R38, their rate constant at 1100 K is an order of magnitude higher than what we have used, but the contribution of R38 is negligible in our experiments. Davidson and co-workers have compiled and revised kinetic parameters for methane and ethane decomposition reactions, especially reactions R15 and R17.[58] For reaction R17, their value has been used, and it is in close agreement with Lim and Michael.[70] They have also shown that reaction R16 is not important at all. The rate constant that we have used for reaction R16 in comparison to reactions R15 and R17 is much smaller and so this would not seriously affect our conclusion. However, for reaction R15, the rate constant of Davidson and co-workers is 2.2 times larger than that given in Table 2, and we suspect that using these rate constants may improve the agreement between simulation and experiment, especially for C_2H_6. Michael and co-workers[71] have reported direct measurements for reaction R41, which is 5 times smaller than what we have used. Hidaka et al.[72−74] have also reported some revised rate constants for reactions R17, R39, and R41. None of these rate parameters are directly determined in this work, and they affect the minor products only. Hence, major conclusions from this work, that is, rate constants for reactions R1 and R2 are unlikely to be affected.

IV. Computational Results and Discussions

Our main objective in the computational work was to identify the transition states for HF and H_2O elimination and estimate the preexponential factor and activation energy for the processes using conventional transition-state theory. For this reason, both ground-state and the transition-state structures were fully optimized at **HF**, MP2(FULL), and DFT(B3LYP) levels with the standard 6-31G*, 6-31G**, 6-31+G**, and 6-311++G** basis sets. Our attempts to get the transition state for HOF elimination were not successful. The FEOH has five rotational isomers due to single-bond rotation about both C−C and C−O bonds, and there have been numerous discussions on their structures, vibrational frequencies, and relative energies.[24−26] The $G_{g'}$ structure is reported[24] to be the most stable structure compared to other forms of 2-fluoroethanol, namely, G_g, G_t, T_g, and T_t (G and T refer to gauche and trans geometry for rotation about the C−C bond and g and t refer to gauche and trans about the C−O bond. For gauche geometry about C−O bond, g′ has the OH proton on the F side enabling hydrogen bonding and g has the OH proton on the other side). The other four conformers have more or less the same energy (within 1 kcal mol^{-1}) according to the best theoretical results available,

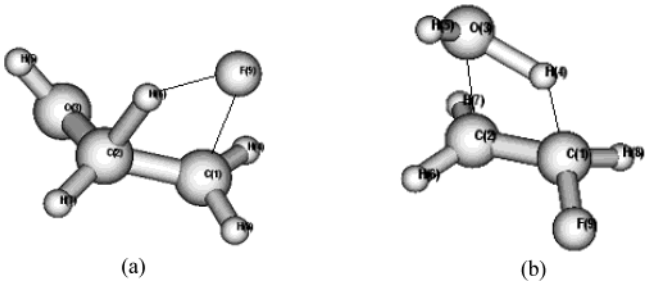

Figure 6. Optimized structures of the transition state for (a) HF elimination and (b) H_2O elimination from 2-fluoroethanol at B3LYP/6-311++G**.

all of them 3−4 kcal mol^{-1} higher than the $G_{g'}$ isomer depending on the level of theory used. Because our main emphasis is on the high-barrier chemical reactions, we consider the global minimum $G_{g'}$ to represent the reactant. Initially, extensive calculations were done for T_t and G_t conformers as well, and our results are in good agreement with earlier published work. To verify the β-substitution effect of F on the barrier for H_2O elimination, calculations were carried out for ethyl alcohol as well. These results are compared with our experimental results.

The fully optimized structures of $G_{g'}$, G_t, and T_t conformers are available on request from the authors, and they are available elsewhere[24−26] as well. Our results are in complete agreement with earlier reports at similar levels of theory. The complete TS structures for HF elimination and H_2O elimination are given in Tables IS and IIS (Tables *X*S are to be found in Supporting Information). To the best of our knowledge, there is no prior report on these structures for comparison. The TS structures for ethyl fluoride (HF elimination)[15] and ethanol (H_2O elimination)[22,23] have been reported, and they are used for comparison with our results. Figure 6 shows structures of the transition states of both HF and H_2O eliminations at B3LYP/6-311++G** level. The TS for HX elimination from ethyl chloride and ethyl fluoride have an effective plane of symmetry that contains all of the four atoms (H, C, C, and X) directly involved in the reaction, that is, the dihedral angle HCCX is zero.[2] For FEOH, the HF elimination TS is not planar with ∠FCCH dihedral angle around 6°−7° at all levels of theory. Similarly, for the TS for H_2O elimination, the ∠OCCH dihedral angle is around 4°−5° at **HF** and MP2 levels, but at DFT (B3LYP) level, it is 1°−3°. It appears that the β-substitution of F/OH distorts the planar TS slightly. Other structural details for both the TSs are described separately next.

IV.A. Transition State for HF Elimination from FEOH. Four bond distances are important at the TS for HF elimination, that is, the newly partially formed C═C and H−X and the breaking C−X and C−H bonds. These have been considered extensively by several workers, and the recent paper by Holmes and co-workers gives a good summary.[44] At the TS, the C−C bond distance at **HF** level is 1.393 Å with 6-31G** basis set, and adding the diffuse functions (6-311++G**) decreases it to 1.388 Å. Adding electron correlation results in an increase in C−C bond length, and it is 1.400 Å at both MP2(FULL)/6-311++G** and B3LYP/6-311++G** levels. This C−C bond distance corresponds to a bond order of ∼1.5, which is very close to that of benzene. It is very similar to the TS found for HF elimination from ethyl fluoride[15] and trifluoroethane[44] as well. The C−F and C−H (the hydrogen that is involved in the HF elimination) bond distances follow a similar trend. At the lowest level of calculations reported here, that is, **HF**/6-31G**, they are 1.927 and 1.303 Å, respectively. Improving the basis set to triple-ζ with polarization functions (6-311++G**) at the **HF** level changes these distances in one direction (2.055 and 1.250 Å), but inclusion of electron correlation brings them back closer to the **HF**/6-31G** predictions. The C−F distance is 1.983 Å at B3LYP/(6-311++G**) and 1.895 Å at MP2(FULL)/(6-311++G**). The C−H distance is 1.310 Å at MP2(FULL)/(6-311++G**) and 1.293 Å at B3LYP/(6-311++G**). The H−F bond distances are very different at different level of calculations. With 6-311++G** basis set, **HF**, MP2, and B3LYP calculations lead to H−F distances of 1.390, 1.313, and 1.362 Å. At all levels, these distances are significantly larger than that of the free HF molecule (0.918 Å). However, unimolecular HX elimination reactions do not lead to significant energy release in the HX vibrational mode.[45] All of these four distances show very similar trend for HF elimination from ethyl fluoride and trifluoroethane as well.[44] It appears that the transition states for HF elimination from ethyl fluoride and other substituted fluoroethanes are very similar in nature.

B. Transition State for H_2O Elimination. The TS for H_2O elimination has longer C−C and C−H bond distances and shorter H−X and C−X distances (X = O/F) compared to that of HF elimination at all levels, though the difference is smaller at the higher level calculations. These changes point to a subtle difference in the four-center transition states for HF and H_2O elimination reactions. Table 3 gives a compact summary of these distances. In particular, the C−H bond is significantly longer at the TS for H_2O elimination than that for the HF elimination. As a result, the H−O bond is more fully formed in H_2O elimination than the H−F bond in HF elimination. It is clearly shown in Figure 6. Butkovskaya and Setser[46] have pointed out such a trend between HF elimination and H_2O elimination from ethyl fluoride and ethanol, respectively. Our results show that 2-fluoroethanol is a good example to identify this trend within the same molecule. In the past, the TS for HX elimination has been characterized as "loose" or "tight" depending primarily on the C−X distance. Looking at the C−O and C−F bond distances, it is clear that the TS for H_2O elimination is tighter than that of HF elimination. It affects the preexponential factor significantly and will be discussed in detail in the next section.

C. TST Calculations. Frequency calculations were carried out at all levels of calculations for both the ground and transition states to perform TST calculations. The ground-state frequencies have been reported earlier by others and are also available from the authors on request. Tables IIIS and IVS list the frequencies at various levels for the transition states of HF and H_2O elimination. The transition states are characterized by one imaginary frequency corresponding to the reaction coordinate. The reaction coordinate corresponds to the motion of H away from C toward F/O in both cases. The motion along the reaction coordinate is very similar to that described by Holmes and co-workers for the HF elimination reaction of CF_3CH_3.[42] The motion of the reaction coordinate when visualized with Molden[47] clearly shows that the transition state corresponds to the reaction of interest.

The thermal rate constants for both HF and H_2O elimination from 2-fluoroethanol were calculated using the transition -state theory expression.[48]

$$k(T) = l\frac{k_B T}{h}\frac{Q_{\neq}}{Q_R}\exp\left[-\frac{E_0}{RT}\right] \qquad (2)$$

where l is the reaction path degeneracy, k_B is the Boltzmann constant, $Q_{\neq}$ and Q_R are partition functions for the transition state and reactant, respectively, and E_0 is the zero-point barrier for the reaction. The thermodynamic formulation of TST is then

TABLE 3: Summary of C−C, C−X, C−H, and H−X Distances and Percent Changes Calculated for the Transition States for HF/H_2O Elimination Reactions from 2-Fluoroethanol[a]

bond (HX)	**HF**/6-31G**	**HF**/6-311++G**	MP2/6-31G**	MP2/6-311++G**	B3LYP/6-31G**	B3LYP/6-311++G**
C−C (HF)	1.393 (−7.8)	1.388 (−8.2)	1.397 (−7.4)	1.400 (−7.5)	1.406 (−7.4)	1.399 (−7.8)
C−C (H_2O)	1.442 (−4.6)	1.457 (−3.4)	1.412 (−6.4)	1.412 (−6.7)	1.421 (−6.5)	1.411 (−7.0)
C−F (HF)	1.944 (+41.9)	2.055 (+50.0)	1.854 (+30.5)	1.895 (+33.4)	1.900 (+36.7)	1.983 (+42.7)
C−O (H_2O)	1.702 (+21.7)	1.629 (+16.4)	1.803 (+26.9)	1.787 (+25.8)	1.845 (+29.9)	1.900 (+29.9)
C−H (HF)	1.305 (+20.0)	1.250 (+15.0)	1.349 (+23.5)	1.310 (+19.6)	1.346 (+22.4)	1.293 (+18.0)
C−H (H_2O)	1.588 (+46.1)	1.645 (+51.3)	1.494 (+36.8)	1.497 (+36.7)	1.467 (+33.4)	1.412 (+28.8)
HF (HF)	1.271 (+41.7)	1.390 (+55.0)	1.245 (+35.2)	1.313 (+42.6)	1.267 (+37.7)	1.362 (+48.0)
HO (H_2O)	1.100 (+16.9)	1.078 (+14.6)	1.196 (+24.9)	1.195 (+24.9)	1.227 (+27.5)	1.268 (+31.8)

[a] For C−C, C−X, and C−H bonds, the percent changes (in parentheses) give the change in these distances compared to the reactant. For the H−X bond, percent change gives the change compared to free HF and H_2O.

TABLE 4: Comparison of the Rate Parameters for the Unimolecular Elimination of HF and H_2O from 2-Fluoroethanol and H_2O Elimination from Ethyl Alcohol[a]

	$FCH_2CH_2OH \rightarrow HF + CH_3CHO$		$FCH_2CH_2OH \rightarrow H_2O + CH_2CHF$		$C_2H_5OH \rightarrow H_2O + C_2H_4$	
theory/basis set	log A	E_a (kcal mol^{-1})	log A	E_a (kcal mol^{-1})	log A	E_a (kcal mol^{-1})
HF/6-311++G**	14.726 ± 0.006	77.72 ± 0.03	14.318 ± 0.005	92.43 ± 0.02	15.700 ± 0.006	85.95 ± 0.01
MP2(FULL)/6-311++G**	14.635 ± 0.006	65.64 ± 0.02	14.721 ± 0.006	75.52 ± 0.03	14.448 ± 0.006	68.87 ± 0.01
B3LYP/6-311++G**	14.532 ± 0.005	58.91 ± 0.02	14.714 ± 0.006	70.07 ± 0.03	14.885 ± 0.006	64.61 ± 0.01
Experiment[b]	13.178 ± 0.14	59.45 ± 1.7	14.302 ± 0.13	69.69 ± 1.7	13.84	67.9

[a] The E_0 values are 74.69, 62.61, and 56.13 kcal mol^{-1} at **HF**, MP2, and DFT levels for HF elimination, respectively. For H_2O elimination, the corresponding values are 89.69, 72.17, and 66.80 kcal mol^{-1}. The entropy of activation, $\Delta S^{\ddagger}$, at 1100 K are 2.9, 2.5, and 2.01 cal K^{-1} mol^{-1} for HF elimination at **HF**, MP2, and DFT levels, respectively. For H_2O elimination, the corresponding values are 1.0, 2.9, and 2.8 cal K^{-1} mol^{-1}. [b] FEOH data is from present work and ethanol data is from ref 22. Butkovskaya et al.[23] quote $A = 10^{14.4}$ and $E_a = 69.2$ kcal mol^{-1} at 1100 K.

used to estimate the E_a and A based on theory.[48] The rate constant for a unimolecular reaction is given by

$$k = le\frac{k_B T}{h}\exp\left[\frac{\Delta S^{\ddagger}}{R}\right]\exp\left[-\frac{E_a}{RT}\right] \qquad (3)$$

Here, $\Delta S^{\ddagger}$ is the entropy of activation calculated using the partition functions of reactant and the transition state. The A and E_a were calculated between 1000 and 1200 K (at 50 K intervals) using the **HF**, MP2(FULL), and DFT results using the largest basis set, 6-311++G**, and average values for this temperature range were estimated. These parameters could be determined by empirically fitting the rate constants, $k(T)$, to the Arrhenius expression. The fit was excellent for all cases suggesting that the Arrhenius expression is valid within this temperature range, and it yielded results in agreement with eqs 2 and 3. The same method is followed for H_2O elimination from ethanol. All of these results are compiled in Table 4. The experimentally obtained values in the present work are also included for the comparison.

At all levels, theory predicts the correct order for activation energies for the two elimination reactions considered here. The E_a for H_2O elimination is significantly higher than that for HF elimination. The agreement between experimental activation energies for both HF and H_2O elimination and the DFT predictions appears too good to be true. It may be noted that Holmes and co-workers have concluded that DFT level theory gives good results for HF elimination reactions.[44] In this particular case, it should be emphasized that FEOH has several other conformers that are higher in energy by 3 kcal mol^{-1}. If their contributions are included, the effective activation energy calculated will be slightly smaller. For HCl elimination from ethyl chloride and 1,2-dichloroethane, it was found that the DFT predictions were underestimating the activation energy.[2] Our results on ethanol appear similar with the DFT calculations underestimating the activation energy. In any case, the **HF** and MP2(FULL) level theories differ from experimental values more significantly, overestimating the barrier by 18 and 6 kcal mol^{-1} for hydrogen fluoride elimination and 13 and 6 kcal mol^{-1} for H_2O elimination from 2-fluoroethanol, respectively.

The activation energy for HF elimination from ethyl fluoride[49] is 59.5 ± 1 kcal mol^{-1}. This estimate is also from single pulse shock tube studies at the same temperature range (996−1137 K). It is nearly the same as that for FEOH, that is, OH substitution does not seem to have increased the activation energy for HF elimination. However, theoretical calculations at all three levels predict an increase of 1−4 kcal mol^{-1} on OH substitution. The activation energy for HF elimination from CH_3CH_2F at **HF**, MP2, and DFT levels with 6-311++G** basis sets are 74.1, 62.3, and 57.5 kcal mol^{-1}, respectively.[75] These values can be compared to those for HF elimination from FEOH at similar levels, 77.7, 65.6, and 58.9 kcal mol^{-1}. Similarly, between ethanol and FEOH, all levels of theory predict an increase of 6−7 kcal mol^{-1} in barrier for H_2O elimination on F substitution. Direct experimental results on the activation energy for H_2O elimination from ethanol are still unavailable, and the results given in Table 4 are predictions from electronic structure and TST calculations.

The preexponential factors (A) estimated by all levels of theory are significantly larger than the experimental observation in our temperature range, especially for HF elimination reaction. At the **HF** level of theory, the TS for HF elimination was significantly looser than that of H_2O elimination, and this is evident from the preexponential factors listed in Table 4. For HF elimination from CF_3CH_3, Holmes and co-workers pointed out that the experimental and theoretical preexponential factors are in good agreement at 800 K.[44] Our results show that the experimental value for HF elimination from FEOH is significantly smaller than theoretical predictions at 1100 K. On the other hand, it appears that the calculated preexponential factors are in good agreement for H_2O elimination at 1000−1200 K. However, one needs to be very cautious in comparing the experimental and theoretical preexponential factors. First, FEOH has two internal rotors that have been treated as harmonic oscillators in our model. Chuang and Truhlar have clearly shown that the partition functions for the hindered rotors can vary by

orders of magnitude depending on the model.[50] At 1100 K, though, harmonic oscillator partition functions are closer to the partition functions calculated more rigorously. For example, for CH_2FCH_2Cl at 1100 K, the partition functions are 5.9, 41.5, and 8.8 for the harmonic oscillator, free rotor, and hindered rotor models, respectively.

McGrath and Rowland have pointed out the importance of tunneling in the HCl elimination reaction from ethyl chloride.[51] However, for comparison with experimental data between 700 and 800 K,[52] they considered the rate constant directly and did not try to fit the preexponential factor and activation energy independently. The experimental activation energy was 56.3 ± 0.3 kcal mol^{-1}, and they were able to fit the rate constants accurately with a calculated classical barrier of 62.7 ± 0.4 kcal mol^{-1}. We note that the rate constant calculated at the MP2 level is in good agreement with the experimental value for HF elimination from FEOH between 1000 and 1100 K because both the preexponential factor and activation energy are larger compared to experiment. For HF and HCl elimination from CH_2FCH_2Cl also, similar agreement between experimental and theoretical rate constants has been noted, though both A and E_a differed significantly between theory and experiment.[75] Certainly, there is a need for more experimental and theoretical work on these reactions covering a wider temperature range for proper understanding of the kinetic parameters.

As mentioned earlier, our attempts to identify the transition state for HOF elimination were not successful. Recently, Zhu and Bozzelli[76] considered Cl_2 elimination reaction from CH_2Cl-CH_2Cl and determined the barrier to be very large, 91.5 kcal mol^{-1} at B3LYP/6-31++G** level. Our results[75] on ClF elimination from CH_2F-CH_2Cl gave a barrier of 145 kcal mol^{-1} at **HF**/6-311++G** level. These results imply that the HOF elimination from FEOH is unlikely and C−O bond dissociation may be the route to C_2H_4 formation. However, direct observation (or the lack of it) of HOF can resolve this question unambiguously.

V. Conclusions

The thermal decomposition of 2-fluoroethanol has been studied in the temperature range of 1000−1200 K. The unimolecular elimination reactions of HF and H_2O have been reported both experimentally and theoretically. Both ab initio and DFT methods have been employed to characterize all of the transition states and ground states. The TST calculations have been performed to obtain the rate parameters for all of the unimolecular elimination processes. From the experimental results, the rate constants for HF, H_2O, and HOF eliminations are estimated to be $10^{13.17\pm0.33}$ exp[−(59.5 ± 1.7)/(RT)], $10^{14.30\pm0.13}$ exp[−(69.7 ± 1.7)/(RT)], and $10^{17.30\pm0.66}$ exp[−(85.9 ± 3.4)/(RT)] respectively. The overall decomposition rate constant is given by $10^{13.55\pm0.32}$ exp[−(60.6 ± 1.6)/(RT)]. The activation energies calculated for HF elimination at **HF**, MP2(FULL), and DFT methods with 6-311++G** basis set differ from the experimental values by +18.2, +6.1, and −0.6 kcal mol^{-1}, respectively. The activation energies for H_2O elimination at the same levels of theory differ from experimental values by 22.7, 5.9, and 0.4 kcal mol^{-1}. Our attempts to get the transition-state structure for HOF elimination at all levels of theories were not successful. Ethylene formation could be explained by considering C−O bond dissociation equally well. Direct real-time spectroscopic observation of HOF would be needed to choose between the two pathways.

Acknowledgment. We acknowledge the financial support from IISc-ISRO Space Technology Cell and the Director, Indian Institute of Science. We also acknowledge Dr. R. B Sunoj of The Ohio State University, Columbus, OH, for fruitful discussions in running Gaussian 94. Mr. D. Anandraj is acknowledged for his help in the experiments. Prof. D. W. Setser is acknowledged for comments on an earlier version. An anonymous referee is acknowledged for critical comments that were helpful.

Supporting Information Available: Four tables containing the optimized transition-state structures for HF and H_2O elimination and the normal-mode frequencies for both transition-state structures for **HF**, MP2(FULL), and DFT (B3LYP) calculations with 6-31G*, 6-31G**, 6-31+G**, and 6-311++G** basis sets. This material is available free of charge via the Internet at http://pubs.acs.org. The completely optimized structures and the normal mode vibrational frequencies of both ground and transition state for H_2O elimination of ethyl alcohol can be obtained from the authors on request.

References and Notes

(1) Kelly, T.; Manning, M.; Bonard, A.; Wenger, J.; Treacy, J.; Sidebottom, H. In *Transport and Chemical Transformation in the Troposphere, Proceedings of EUROTRAC Symposium 2000, 6th*; Garmisch-Partenkirchen, Germany, 27−31 March, 2000; Midgley, P. M., Reuther, M., Williams, M., Eds.; Springer: Berlin, 2001; pp 410−413.
(2) Rajakumar, B.; Reddy, K. P. J.; Arunan, E. *J. Phys. Chem. A* **2002**, *106*, 8366.
(3) Maccoll, A. *Chem. Rev.* **1969**, *69*, 33.
(4) Cadman, P.; Day, M.; Trotman-Dickenson, A. F. *J. Chem. Soc. A* **1971**, 1356.
(5) Evans, P. J.; Ichimura, T.; Tschuikow-Roux, E. *Int. J. Chem. Kinet.* **1978**, *10*, 855.
(6) Weissman, M.; Benson, S. W. *Int. J. Chem. Kinet.* **1984**, *16*, 941.
(7) Jones, Y.; Holmes, B. E.; Duke, D. W.; Tipton, D. L. *J. Phys. Chem.* **1990**, *94*, 4957.
(8) Rakestraw, D. J.; Holmes, B. E. *J. Phys. Chem.* **1991**, *95*, 3968.
(9) McDoniel, J. B.; Holmes, B. E. *J. Phys. Chem.* **1996**, *100*, 3044.
(10) Srivatsa, A.; Arunan, E.; Manke, G., II; Setser, D. W.; Sumathi, R. *J. Phys. Chem. A.* **1998**, *102*, 6412.
(11) Sudbo, Aa. S.; Schulz, P. A.; Shen, Y. R.; Lee, Y. T. *J. Chem. Phys.* **1978**, *69*, 2312.
(12) Quick C. R.; Wittig, C. *J. Chem. Phys.* **1980**, *72*, 1694.
(13) Tsang, W. *J. Chem. Phys.* **1964**, *41*, 2487.
(14) Skingle, D. C.; Stimson, V. R. *Aust. J. Chem.* **1976**, *29*, 609.
(15) Toto, J. L.; Pritchard, G. O.; Kirtman, B. *J. Phys. Chem.* **1994**, *98*, 8359.
(16) Chuchani, G.; Martin, I.; Rotinov, A.; Hernandez, A.; Reikonnen, N. *J. Phys. Chem.* **1984**, *88*, 1563.
(17) Borisov, A. A.; Zamanskii, V. M.; Konnov, A. A.; Lisyanskii. V. V.; Rusakov, S. A.; Skachkov, G. I. *Sov. J. Chem. Phys.* **1992**, *9*, 2527.
(18) Natarajan, K.; Bhaskaran, A. *Proc. 13th Int. Shock Tube Symp.* **1981**, 834.
(19) Li, J.; Kazakov, A.; Dryer, F. L. *Int. J. Chem. Kinet.* **2001**, *33*, 859.
(20) Dunphy, M. P.; Patterson, P. M.; Simmie, J. M. *J. Chem. Soc., Faraday Trans.* **1991**, *87*, 2549.
(21) Marinov, N. M. *Int. J. Chem. Kinet.* **1999**, *31*, 183.
(22) Park, J.; Zhu, R. S.; Lin, M. C. *J. Chem. Phys.* **2002**, *117*, 3224.
(23) Butkovskaya, N. I.; Zhao, Y.; Setser, D. W. *J. Phys. Chem.* **1994**, *98*, 10779.
(24) Gounev, T. K.; Bell, S.; Zhou, L.; Durig, J. R. *J. Mol. Struct.* **1998**, *447*, 21.
(25) Buemi, G. *J. Chem. Soc., Faraday Trans.* **1994**, *90*, 1211.
(26) Dixon, D. A.; Smart, B. E. *J. Phys. Chem.* **1991**, *95*, 1609.
(27) McWhorter, D. A.; Hudspeth, E.; Pate, B. H. *J. Chem. Phys.* **1999**, *110*, 2000.
(28) Green, D.; Hammond, S.; Keske, J.; Pate, B. H. *J. Chem. Phys.* **1999**, *110*, 1979.
(29) Rasanen, M.; Murto, J.; Bondeybey, V. E. *J. Phys. Chem.* **1985**, *89*, 3967.
(30) Shirk, J. S.; Marquardt, C. L. *J. Chem. Phys.* **1990**, *92*, 7234.
(31) Brummel, C. L.; Mork, S. W.; Philips, L. A. *J. Chem. Phys.* **1991**, *95*, 7041.
(32) Frisch, M. J.; Trucks, G. W.; Schlegel, H. B.; Gill, P. M. W.; Johnson, B. G.; Robb, M. A.; Cheeseman, J. R.; Keith, T.; Petersson, G. A.; Montgomery, J. A.; Raghavachari, K.; Al-Laham, M. A.; Zakrzewski, V. G.; Ortiz, J. V.; Foresman, J. B.; Cioslowski, J.; Stefanov, B. B.; Nanayakkara, A.; Challacombe, M.; Peng, C. Y.; Ayala, P. Y.; Chen, W.;

Wong, M. W.; Andres, J. L.; Replogle, E. S.; Gomperts, R.; Martin, R. L.; Fox, D. J.; Binkley, J. S.; Defrees, D. J.; Baker, J.; Stewart, J. P.; Head-Gordon, M.; Gonzalez, C.; Pople, J. A. *Gaussian 94*, revision C.2; Gaussian, Inc.: Pittsburgh, PA, 1995.

(33) Zhang, Y.-X.; Bauer, S. H. *J. Phys. Chem. B* **1997**, *101*, 8717.

(34) Kern, R. D.; Singh, H. J.; Xie, K. *AIP Conf. Proc. (Curr. Top. Shock Waves)* **1990**, 487.

(35) Martell, J. M.; Yu, H.; Goddard, J. D. *Mol. Phys.* **1997**, *92*, 497.

(36) Cioslowski, J.; Schimeczek, M.; Liu, G.; Stoyanov, V. *J. Chem. Phys.* **2000**, *113*, 9377.

(37) Suenobu, K.; Nagaoka, M.; Yamabe, T. *J. Mol. Struct. (THEOCHEM)* **1999**, *461*−*462*, 581.

(38) Lifshitz, A.; Ben-Hamou, H. *J. Phys. Chem.* **1983**, *87*, 1782.

(39) Cadman, P.; Engelbrecht, W. J. *Chem. Commun*. **1970**, 453.

(40) Gray, P.; Herod, A. A. *Trans. Faraday Soc*. **1968**, *64*, 1568.

(41) McMillen, D. F.; Golden, D. M. *Annu. Rev. Phys. Chem*. **1982**, *33*, 493.

(42) Klaassen, J. J.; Linder, J.; Leone, S. R. *J. Chem. Phys*. **1996**, *104*, 7403.

(43) Marcy, P. T.; Reid, J. P.; Qian, C. X. W.; Leone, S. R. *J. Chem. Phys*. **2001**, *114*, 2251.

(44) Martell, J. M.; Beaton, P. T.; Holmes, B. E. *J. Phys. Chem. A* **2002**, *106*, 8471.

(45) Arunan, E.; Wategaonkar, S. J.; Setser, D. W. *J. Phys. Chem.* **1991**, *95*, 1539.

(46) Butkovskaya, N. I.; Setser, D. W. *J. Chem. Phys.* **1996**, *105*, 8064.

(47) Schaftenaar, G.; Noordik, J. H. Molden: a pre- and postprocessing program for molecular and electronic structures. *J. Comput.-Aided Mol. Des.* **2000**, *14*, 123.

(48) Wright, M. R. *Fundamental Chemical Kinetics: An exploratory introduction to the concepts;* Horwood Publishing: Chichester, U.K., 1999.

(49) Okada, K.; Tschuikow-Roux, E.; Evans, P. J. *J. Phys. Chem.* **1980**, *84*, 467.

(50) Chuang, Y.-Y.; Truhlar, D. G. *J. Chem. Phys.* **2000**, *112*, 1221.

(51) McGrath, M. P.; Rowland, F. S. *J. Phys. Chem. A* **2002**, *106*, 8191.

(52) Heydtmann, H.; Dill, B.; Jonas, R. *Int. J. Chem. Kinet.* **1975**, *7*, 973.

(53) Lifshitz, A.; Tamburu, C.; Suslensky, A. *J. Phys. Chem.* **1990**, *94*, 2966.

(54) Tsang, W.; Hampson, R. P. *J. Phys. Chem. Ref. Data* **1986**, *15*, 1087.

(55) Baulch, D. L.; Cobos, C. J.; Cox, R. A.; Esser, C.; Frank, P.; Just, Th.; Kerr, J. A.; Pilling, M. J.; Troe, J.; Walker, R. W.; Warnatz, J. *J. Phys. Chem. Ref. Data* **1992**, *21*, 411.

(56) Colket, M. B., III; Naegeli, D. W.; Glassmann, I. *Int. J. Chem. Kinet.* **1975**, *7*, 223.

(57) Kern, R. D.; Singh, H. J.; Wu, C. H. *Int. J. Chem. Kinet.* **1988**, *20*, 731.

(58) Davidson, D. F.; DiRosa, M. D.; Chang, E. J.; Hanson, R. K.; Bowman, C. T. *Int. J. Chem. Kinet.* **1995**, *27*, 1179.

(59) Warnatz, J. In *Combustion Chemistry*; Gardiner, W. C., Jr., Ed.; Springer-Verlag: New York, 1984; p 197.

(60) Frank, P.; Bhaskaran, K. A.; Just, Th. *J. Phys. Chem.* **1986**, *90*, 2226.

(61) Frank, P.; Just, Th. *Proc. Int. Symp. Shock Tubes and Waves* **1984**, *14*, 706.

(62) Mackie, J. C.; Doolan, K. R. *Int. J. Chem. Kinet*. **1984**, *16*, 525.

(63) Diau, E. W.-G.; Lee, Y.-P. *J. Chem. Phys.* **1992** *96*, 377.

(64) Fagerstrom, K.; Lund, A.; Mahmoud, G.; Jodkowski, J. T.; Ratajczak, E. *Chem. Phys. Lett*. **1993**, *208*, 321.

(65) Barat, R. B.; Bozzelli, J. W. *J. Phys. Chem.* **1992**, *96*, 2494.

(66) Park, C. *J. Phys. Chem.* **1977**, *81*, 499.

(67) Kondratev, V. N. *Kinet. Catal.* **1961**, *8*, 831.

(68) Lloyd, A. C. *Int. J. Chem. Kinet.* **1971**, *3*, 39.

(69) Sutherland, J. W.; Su, M.-C.; Michael, J. V. *Int. J. Chem. Kinet.* **2001**, *33*, 669.

(70) Lim, K. P.; Michael, J. V. *25th Symp. (Int.) Combust.* **1994**, 713.

(71) Hranisavljevic, J.; Kumaran, S. S.; Michael, J. V. *27th Symp. (Int.) Combust*. **1998**, 159.

(72) Hidaka, Y.; Sato, K.; Henmi, Y.; Tanaka, H.; Inami, K. *Combust. Flame* **1999**, *118*, 340.

(73) Hidaka, Y.; Sato, K.; Hoshikawa, H.; Nishimori, T.; Takahashi, R.; Tanaka, H.; Inami,; Ito, N. *Combust. Flame* **2000**, *120*, 245.

(74) Hidaka, Y.; Kimura, K.; Kawano, H. *Combust. Flame* **1994**, *99*, 18.

(75) Rajakumar, B.; Arunan, E. *Phys. Chem. Chem. Phys.* **2003**, *5*, 3897.

(76) Zhu, L.; Bozzelli, J. W. *Chem. Phys. Lett.* **2002**, *357*, 65.